New high resolution geochemistry of Lower Jurassic marine sections in western North America: A global positive carbon isotope excursion in the Sinemurian?

Sarah J. Porter [a,b,c]*, Paul L. Smith [a], Andrew H. Caruthers [a], Pengfei Hou [a], Darren R. Gröcke [b] and David Selby [b]

[a] Department of Earth, Ocean and Atmospheric Sciences, University of British Columbia, V6T 1Z4, Canada.
[b] Department of Earth Sciences, University of Durham, Durham, DH1 3LE, UK.
[c] Chemostrat Ltd., Unit 1 Ravenscroft Court, Buttington Cross Enterprise Park, Welshpool, Powys, SY21 8SL, UK.

*Corresponding author. Email: sarahporter@chemostrat.com

Abstract

Recognising variations in the carbon isotope compositions of marine organic-rich sedimentary rocks can provide insight into changes in ocean chemistry throughout geological time. Further, identification of global excursions in the carbon isotope record has proved to be valuable as a chronostratigraphic correlation tool.

This investigation presents new high-resolution organic carbon isotope data ($\delta^{13}C_{org}$) for marine sediments from 2 regions in North America (Last Creek, British Columbia, Canada and Five Card Draw, Nevada, USA). The carbon isotope profiles demonstrate that there were significant differences between the carbon reservoirs at Five Card Draw and Last Creek, notably in the upper part of the Leslei Zone. The $\delta^{13}C_{org}$ values show a gradual positive CIE (~2 ‰) at Last Creek in the upper part of the Leslei Zone. This corresponds to a coeval positive CIE of similar duration in Dorset, UK (upper Turneri Zone; Jenkyns and Weedon, 2013), suggesting that this may be a global marine carbon isotope signature, and likely reflects a widespread increase in primary productivity during the Early Sinemurian. In addition, a brief negative CIE is observed in the uppermost Lower Sinemurian at Last Creek. This negative excursion is not recorded in the Dorset section, suggesting localised upwelling of ^{12}C-rich bottom-waters at Last Creek. Further, the signals identified at Last Creek are not present in coeval sections at Five Card Draw, thus highlighting a significant difference between these localities. Osmium (Os) isotope data (initial $^{187}Os/^{188}Os$ values) provide a quantitative determination of the contrasting depositional environments of Five Card Draw and Last Creek (at least partially restricted with high levels of continental inundation and open-ocean, respectively). This demonstrates that basinal restriction may act as a major factor that controls isotopic stratigraphic signatures, thus preventing the identification of global or widespread regional excursions.

Keywords: Stable carbon isotopes, carbon isotope excursions (CIEs), osmium isotopes, Lower Jurassic, Sinemurian, North America.

1. Introduction

Understanding marine sedimentary rocks and their depositional environments throughout geological time allows us to evaluate past changes in ocean chemistry. The ability to recognise these variations, at both the localised and global scale, enables us to trace temporal alterations in the balance of inputs to the global oceans. To do this, geochemical traces such as carbon and osmium (Os) isotopes are utilised. Carbon isotope profiling enables us to detect variations in primary productivity (Hesselbo et al., 2000), together with periods of increased bottom-water upwelling, and widespread oxidation of organic matter during eustatic sea level fall (Jenkyns et al., 2002). Osmium isotopes allow tracing of inorganic fluxes into the marine environment, by recording the effects of meteorite impacts, continental weathering, and volcanogenic fluxes (Cohen et al., 1999; Peucker-Ehrenbrink and Ravizza, 2000).

The Jurassic Period witnessed major tectonic events that significantly impacted the global environment; most notably the global tectonic plate reorganisation associated with the break-up of Pangaea. Early Jurassic Pangaean fragmentation into Laurasia and Gondwana established new seaways and marine connections and was accompanied by a steady rise in sea level (Hallam, 1981). This complex and dynamic tectonic period was also associated with significant fluctuations in global ocean chemistry (Cohen et al., 1999; Hesselbo et al., 2000; Cohen and Coe, 2007; Jenkyns, 2010; Jenkyns and Weedon, 2013; Riding et al., 2013; Porter et al., 2013), resulting from a number of factors including increased tectonism.

The identification of global carbon isotope excursions (CIEs) throughout geological time significantly improves our ability to conduct temporal correlations of marine and continental successions. In addition, fluctuations in the marine stable carbon isotope record, on a localised and global scale, enable the recognition of changes in ocean chemistry and the evaluation of variations in the balance of inputs to the global oceans through time. A number of previous workers have recognised oceanic carbon isotope excursions (CIEs) during the Early Jurassic, as both global and smaller-scale events. Widespread attention has been given to the negative CIE during the Early Toarcian oceanic anoxic event (T-OAE at ~182 Ma; Hesselbo et al., 2000; Cohen and Coe, 2007; McArthur et al., 2008; Jenkyns, 2010; Caruthers et al., 2011), that is hypothesised to have resulted from the release of ^{12}C-enriched methane accumulated below the seafloor (Hesselbo et al., 2000; Cohen and Coe, 2007). Other negative CIEs have also been reported across both the Pliensbachian-Toarcian boundary (Hesselbo et al., 2007) and the Sinemurian-Pliensbachian boundary (Korte and Hesselbo, 2011). However, until recently the Sinemurian time interval has remained poorly understood. Work in the UK

(Jenkyns and Weedon, 2013 and Riding et al., 2013) has highlighted carbon isotope anomalies in the Sinemurian marine and terrestrial records, but it is not clear from these investigations whether or not these anomalies represent a global signal.

Herein, we present high-resolution carbon isotope data for Sinemurian marine sections from Five Card Draw, Nevada, USA (Taylor et al., 1983; 2001) and Last Creek, British Columbia, Canada (Umhoefer and Tipper, 1998; Smith et al. 1998; Smith and Tipper, 2000; Macchioni et al., 2006) in order to determine whether a global carbon isotope signal can be identified during the Sinemurian. In addition, osmium isotope data is used to quantitatively evaluate differences between the depositional environments of these two North American regions, allowing us to assess how the depositional realm can influence the recording of isotopic anomalies in the stratigraphic record.

2. Geological setting

2.1 Five Card Draw, Nevada, USA

The Sunrise Formation of the Volcano Peak Group cropping out in the Gabbs Valley Range (Fig. 1) is a component of the Pamlico-Luning lithotectonic assemblage of the Walker Lake Terrane (Oldow, 1978; Silberling, 1959; Taylor and Smith, 1992). The formation is part of a platform sequence deposited on basement that had already accreted to western North America by the Jurassic (Fig. 2; Speed, 1979; Taylor and Smith, 1992). The type-section of the Five Card Draw Member of the Sunrise Formation is also the type-section for the Leslei to Harbledownense part of the North American Sinemurian ammonite zonation scheme (Taylor et al., 2001). The section represents a transgressive sequence possibly of eustatic origin (Hallam, 1981), with a depositional environment that ranges from initially shallow, subtidal and moderate to high energy, to offshore deep marine and low energy (Taylor et al., 1983). A low energy basinal setting following eustatic sea-level rise is supported by the analysis and discussion of composite assemblages (organisms that co-occur as a result of environmental factors) by Taylor et al. (1983).

The Five Card Draw Member conformably overlies shallow water limestone beds of the Ferguson Hill Member (Taylor et al., 1983; this study). At its base, the Five Card Draw Member consists of siliceous siltstone and mudstone which transition stratigraphically upwards into darker grey to black mudstones signifying overall a transgressive sequence (Taylor et al., 1983; this study; Fig. 3). The FCD member grades upwards into calcareous siltstone and limestone of the overlying New York Canyon Member.

2.2 Last Creek, British Columbia, Canada

The Last Creek field area is located in the south-eastern Coast Mountains of British Columbia, Canada, approximately 300 km north of Vancouver (Fig. 1). Last Creek is situated within the Cadwallader Terrane, one of a number of pre-Cretaceous terranes that form the Coast Mountains and adjoining areas. The Cadwallader Terrane was founded on Late Palaeozoic oceanic lithosphere (Monger, 2011) and was situated in the north-east corner of the Panthalassa (palaeo-Pacific) Ocean during the Early Jurassic (Fig. 2). It is thought that the Cadwallader and adjacent terranes had amalgamated and accreted to the continent by the Late Jurassic (Monger, 2011).

The Cadwallader Terrane is marine in origin, containing predominantly volcaniclastic sedimentary facies and arc-related volcanic rocks (Monger, 2011). The Last Creek Formation, discussed herein, is a Late Hettangian-Early Bajocian component of these clastic sequences (Schiarizza et al., 1997; Umhoefer and Tipper, 1998). This formation, which is composed of shallow marine coarse clastic rocks with frequently interbedded siltstones that grade upwards into abundant siltstones and marine shales, has been interpreted as a transgressive marine sequence (Macchioni et al., 2006). The lower coarse clastic inner shelf deposits are assigned to the Castle Pass Member, and the deep marine shales to the Little Paradise Member of the Last Creek Formation (Umhoefer and Tipper, 1998; Smith et al., 1998; Smith and Tipper, 2000; this study). The Sinemurian Little Paradise Member exposed at Last Creek consists of finely laminated and fissile black mudstone and siltstone with occasional thin sandstone units (Umhoefer and Tipper, 1998; this study; Fig. 3). In addition, thin (up to 2 cm) yellow-white clay-rich layers are present which may represent ash layers (Umhoefer and Tipper, 1998; Fig. 3).

3. Biochronology

The biochronological constraints in this work use the Sinemurian ammonite zonation for North America established by Taylor et al. (2001) based on successions in the western United States and Mexico, and also incorporating the work of Pálfy et al. (1994) which dealt with successions in Haida Gwaii (former Queen Charlotte Islands) in British Columbia, Canada. The stratigraphic ranges of ammonite genera collected during our study are shown in Figure 4.

Four ammonite zones are recognized in the Five Card Draw section, namely, in ascending stratigraphic order, the Involutum, Leslei, Carinatum, and Harbledownense zones. The Involutum Zone is characterized by the restricted occurrences of *Coroniceras* sp. and *Arnioceras nevadanum*. *Tmaegoceras nudaries*, *Tmaegoceras* sp., *Tipperoceras mullerense* occur in the upper part of the Involutum Zone. The top of the Involutum Zone is the uppermost bed of the Ferguson Hill Member. The Leslei Zone is characterized by an abundance of species of *Arnioceras* including *Arnioceras* cf. *oppeli*, *A.* cf. *mendax*, *A. humboldti*, *A. arnouldi,* and *A. miserabile*. The upper part of the zone is characterized by the occurrences of *Bartoliniceras leslei* (subsequently placed in *Ectocentrites* by Meister et al., 2002) and *Arnioceras laevissimum*. The Carinatum Zone is characterized by the occurrences of *Epophioceras* aff. *carinatum*, *Epophioceras* cf.

bochardi, *Epophioceras* sp., *Asteroceras* sp., and *Asteroceras* cf. *varians*. Some poorly preserved specimens of *Asteroceras* cf. *jamesi* were found in float from this interval. Due to its difficulty in recognition, the Jamesi Zone established by Taylor *et al*. (2001) is provisionally included here as a horizon within the upper part of the Carinatum Zone. The Harbledownense Zone is characterized by the occurrence of abundant echioceratids and rare oxynoticeratids. The base of the zone is characterized by the first appearance of *Paltechioceras harbledownense*.

The two zones recognized in the Last Creek section are the Involutum Zone and Leslei Zone of the Lower Sinemurian. The presence of the Carinatum Zone is indicated by some *ex situ* ammonites from the top of the succession (Macchioni et al., 2006). The Involutum Zone is characterized here by the restricted occurrence of various species of *Coroniceras*, including *Coroniceras* cf. *bisulcatum* and *Coroniceras multicostatum.* The top of the zone is marked by the first appearance of *Arnioceras* cf. *ceratitoides* and the incoming of other *Arnioceras. Tipperoceras* is known from this interval. The lower part of the Leslei Zone is characterized by the restricted occurrences of *Arnioceras* sp., *A.* cf. *ceratitoides*, and *A. miserabile.* The upper part is characterized by the occurrences of *Arnioceras* cf. *humboldti*, *Caenisites brooki*, *C. turneri*, *C. pulchellus*, *Lytotropites fucinii*, *Nevadaphyllites* sp., *Procliviceras striatocostatum* and *Togaticeras* sp. *juv. Arnioceras arnouldi* ranges throughout this zone. A detailed description of the fauna from the upper part of the Leslei Zone in Last Creek is given by Macchioni *et al*. (2006).

The primary standard zonation scheme for the Sinemurian Stage was established by Dean et al. (1961) based on successions in northwest Europe with numerous subsequent refinements summarized in Page (2003) including the work of Cariou and Hantzpergue (1997). The secondary Sinemurian zonation scheme for western North America is correlated with the primary zonation by Taylor et al. (2001) as shown in Figure 4. Radiogenic ages of the Sinemurian Stage show a duration of 8.5 myr, from 199.3 ± 1.0 Ma to 190.8 ± 0.3 Ma (Gradstein et al., 2012). The age of the biozone boundaries have been determined using U-Pb and $^{40}Ar/^{39}Ar$ in the western North

American Cordillera by Pálfy et al. (2000).

4. Sampling

This study focuses on the Sinemurian interval, from the Involutum Zone to the base of the Harbledownense Zone. In each of the two study areas (Five Card Draw, USA and Last Creek, Canada) two sections were profiled (Fig. 3). In total, 520 samples were collected from four field sites for geochemical analysis (total organic carbon – TOC wt. %, stable carbon isotope ratios, and in some cases Re-Os). Total organic carbon and carbon isotope analyses were conducted on all samples, at an average sampling interval of 0.3 m. In addition, 28 of these samples were selected for Re-Os analysis. The Re-Os sampling interval varies and is based upon lithological and biostratigraphical controls.

In Nevada, samples were taken from two measured stratigraphic sections (FCD1 and FCD2) of the Five Card Draw Member of the Sunrise Formation (Taylor et al., 1983; Ferguson and Muller, 1949). The main section (FCD1; Fig. 3) is ~104 m thick and spans the upper part of the Involutum Zone to the Harbledownense Zone. The FCD1 section is the most complete of the sections presented in this study and, as such, it can be used as a reference to correlate all four sections. In total, 259 samples were collected from FCD1 for Total Organic Carbon (TOC) and carbon isotope analysis over the 104 m. This includes samples taken from the Ferguson Hill and Five Card Draw Member transition (Js2-Js3 in the terminology of Ferguson and Muller, 1949). In addition, 11 of these samples were selected for Re-Os isotope analysis over 50 m (within the 25-75 m interval).

The second Five Card Draw section (FCD2) includes the upper 40 m of the Five Card Draw Member from the Carinatum Zone to the base of the Harbledownense Zone, below the Five Card Draw-New York Canyon Member transition (Js3-Js4 in the terminology of Ferguson and Muller, 1949). In total, 80 samples were taken from this section (0-40 m) for TOC and carbon isotope analysis.

The Lower to Middle Jurassic Last Creek Formation is exposed in Last Creek, a tributary of Tyaughton Creek (Fig. 1). The lower section exposed at Last Creek (LC1; Fig. 3) spans the upper part of the Involutum Zone to the lower part of the Leslei Zone (over ~18 m). In total, 61 samples were collected for TOC and carbon isotope analysis, and 9 of these were used for Re-Os isotope analysis. The upper section exposed at Last Creek section (LC2; Fig. 3) spans ~38 m of the Leslei Zone. From this section, 120 samples were taken for TOC and carbon isotope geochemistry, and 8 samples (over ~21 m) were used to conduct Re-Os isotope analysis.

5. Analytical Protocol

Prior to geochemical analyses, the samples were cut and polished, before being powdered and homogenised in either a tungsten disc mill (for TOC and $\delta^{13}C_{org}$) or zirconium disc mill (for Re and Os). Once powdered, samples being analysed for TOC and $\delta^{13}C_{org}$ were decalcified using 45 ml 3N HCl.

5.1 Total Organic Carbon (TOC) and $\delta^{13}C_{org}$

Stable carbon isotope measurements were performed at the University of Durham using a Costech Elemental Analyser (ECS 4010) coupled to a ThermoFinnigan Delta V Advantage. Carbon-isotope ratios are corrected for ^{17}O contribution and reported in standard delta (δ) notation in per mil (‰) relative to the VPDB scale. Data accuracy is monitored through routine analyses of in-house standards, which are stringently calibrated against international standards (e.g., USGS 40, USGS 24, IAEA 600, IAEA CH6): this provides a linear range in $\delta^{13}C$ between +2 ‰ and –47 ‰. Analytical uncertainty for δ^{13}Corg is typically ±0.1 ‰ for replicate analyses of the international standards and typically <0.2 ‰ on replicate sample analysis. Total organic carbon (TOC wt. %) was obtained as part of the isotopic analysis using an internal standard (i.e., Glutamic Acid, 40.82 % C).

5.2 Rhenium and Osmium

Rhenium and osmium abundances and isotopic compositions were obtained in the TOTAL Laboratory for Source Rock Geochronology and Geochemistry, part of the Durham Geochemistry Group, at the University of Durham UK, following the protocol outlined by Selby and Creaser (2003). Sample powders of known quantities (200 to 500 mg) were digested and equilibrated with a measured amount of ^{185}Re and ^{190}Os tracer (spike) solution and 8 ml of CrO_3-H_2SO_4 in Carius tubes at 240^{o}C for 48 hrs. The CrO_3-H_2SO_4 procedure minimises removal of Re and Os from the non-hydrogenous (detrital) component of the sample, allowing analysis and evaluation of the hydrogenous fraction (Selby and Creaser, 2003).

Osmium was removed and purified from the solution by solvent extraction ($CHCl_3$) and micro-distillation techniques. Following Os removal, the remaining solution was prepared for anion exchange chromatography to purify the Re fraction. To reduce Cr^{6+} to Cr^{3+}, necessary to avoid complications during chromatography (Selby and Creaser, 2003), NaOH-acetone solvent extraction was utilised to isolate Re from the CrO_3-H_2SO_4 solution prior to standard HNO_3-HCl anion chromatography (outlined by Cumming et al., 2013).

The purified Re and Os fractions were loaded onto Ni and Pt filaments, respectively and the Re and Os isotope ratios were measured using NTIMS (Creaser et al., 1991; Völkening et al., 1991) using Faraday collectors and the SEM, respectively. Uncertainties presented in Table 1 include full error propagation of uncertainties in Re and Os mass spectrometer measurements, blank abundances and isotopic compositions, spike calibrations and reproducibility of standard Re and Os isotopic values. This sample set was processed at the same time as those of Cumming et al. (2013) which reported total procedural blanks of 4.1 ± 0.03 pg for Re and 0.18 ± 0.07 pg for Os (1 S.D., n = 2), with an average $^{187}Os/^{188}Os$ value of 0.59 ± 0.58. Standard in-house solutions run during the study are 0.5982 ± 0.0015 for $^{185}Re/^{187}Re$ (1 SD; n = 257) and 0.106095 ± 0.00048 for $^{187}Os/^{188}Os$ (1 SD; n = 178).

6. Results

6.1 Total Organic Carbon (TOC) and $\delta^{13}C_{org}$

Measured bulk TOC and $\delta^{13}C_{org}$ data for the Five Card Draw samples are presented in Figure. 5. The TOC concentration is consistently low for both FCD1 and FCD2 sections, with all samples (apart from one) falling within the range of 0.03-2.77 wt. %. The only exception to this is sample FCD1-095 (16.57 wt. % at 38.5 m). Aside from this and some minor peaks up to ~1.70 wt. %, TOC values in FCD1 are relatively consistent (average value of 0.31 wt. %) until ~73 m, where the TOC profile becomes more erratic (average value of 0.8 wt. %). The variability noted here is also reflected in the 0-20 m interval of the FCD2 section (average of 0.78 wt. %). However, from 20-28 m little variability is observed in the TOC values (0.06-0.33 wt. %).

In FCD1, $\delta^{13}C_{org}$ values range from -22 to -26 ‰. In the lowest part of the section (0-20 m), a gradual shift to more negative $\delta^{13}C_{org}$ values is observed, with an average value of -23.85 ‰. For the remainder of the Leslei Zone (~20-73 m), $\delta^{13}C_{org}$ values are relatively consistent with an average value of -25.82 ‰. Following this, a slight rise in $\delta^{13}C_{org}$ (~ 1 ‰) is noted in the Carinatum Zone (~73-100 m). The $\delta^{13}C_{org}$ data for FCD2 is comparable to that of FCD1, with a range of -23.10 to -26.10 ‰ and an average of -24.92 ‰. The gradual 1 ‰ positive shift in the Carinatum Zone seen at FCD1 is also observed in this section.

Total organic carbon and $\delta^{13}C_{org}$ data for the Last Creek sections are presented in Fig. 6. The TOC concentration is generally low in all samples for both LC1 and LC2 sections, ranging from 0.01-3.05 wt. % and 0.18-2.10 wt. %, respectively. Little fluctuation is observed in the lowermost part of LC1 (0-10 m), with all values falling within the range of 0.10-0.86 wt. %. Greater variation is seen from 10-17 m in LC1, with TOC concentrations of 0.32-3.05 wt. %. This variation continues into the base of LC2 (0-8 m; 0.18-2.10 wt. %). Over the 13-20 m interval within LC2, the TOC values decrease from 1.80-0.65 wt. %, before becoming relatively consistent for the remainder of the section (20-38 m), with an average value of 0.65 wt. %.

The $\delta^{13}C_{org}$ data for LC1 falls within the range of -23.28 to -26.28 ‰. There is an initial negative peak at the base of the section (-26.28 ‰; 0.3 m). Following this, $\delta^{13}C_{org}$ values maintain an average of -24.59 ‰ from 0.9-10 m, before shifting to more negative values (average of -25.35 ‰; 10-13 m). At ~13.9 m there is a prominent positive shift to -23.28 ‰, with a subsequent return to values that average -25.57 ‰ for the remainder of the LC1 section.

At the base of LC2 (0-2 m) $\delta^{13}C_{org}$ values average -26.89 ‰, before shifting to more positive values from ~3-13 m with an average value of -25.89 ‰. A positive shift to -24.66 ‰ is also observed within this interval at 6.6 m. Following this, the data gradually shifts from -25.52 ‰ (13.5 m) to -23.66 ‰ (28.6 m). A prominent negative excursion, averaging -26.53 ‰, is observed over a 4.2 m interval at 28.9-33.1 m. At 33.1 m, the carbon isotope values immediately return to an average of -23.95 ‰ for the remainder of the section; comparable to values prior to the negative excursion (-23.90 ‰; 25-28.9 m).

6.2 Rhenium and osmium abundance and isotope data

All measured Re and Os abundances and isotopic compositions for the Five Card Draw and Last Creek sections are presented in Table 1, and Figs. 5 and 6, respectively.

Rhenium and osmium abundances for samples from Five Card Draw range from ~1.5-57 ppb and ~74-577 ppt, respectively, and the $^{187}Re/^{188}Os$ ratio fluctuates between ~97-845. The initial Os isotope composition of the samples ($^{187}Os/^{188}Os_{(i)}$) is extremely variable, with values ranging from ~0.20-2.81. Of the 11 samples, 8 have highly radiogenic values (1.36-2.81), and 5 of these have $^{187}Os/^{188}Os_{(i)}$ greater than 2. These samples contain the lowest levels of Re (1.5-11 ppb). When compared with the stratigraphic column (Fig. 5) and considering the sampling interval, no relationship exists between $^{187}Os/^{188}Os_{(i)}$ and lithology or stratigraphic position.

Samples from LC1 contain ~4.5-18 ppb Re and ~93-144 ppt Os. Values for the $^{187}Re/^{188}Os$ ratio are comparable to those at FCD, varying from ~184-1217. The initial Os isotope ratios are less variable and more unradiogenic than those at FCD, and range between ~0.11-0.48 (Fig. 6).

Sample Re and Os abundances at LC2 are lower than those at FCD and LC1, and range from ~1-10 ppb and ~35-90 ppt, respectively. The $^{187}Re/^{188}Os$ ratios are comparable to those measured at FCD and LC1 (~136-815). Similarly, the $^{187}Os/^{188}Os_{(i)}$ values at LC2 are low in comparison to those from FCD (~0.12-0.91; Fig. 6). As with the samples at Five Card Draw, no trend can be drawn between the initial Os isotope composition of the samples at Last Creek, and their stratigraphic height or lithology.

7. Discussion

7.1 Comparing carbon isotope profiles from Five Card Draw and Last Creek

It is important to note that this study focuses on carbon isotope profiles for bulk organic matter, and does not differentiate between the marine versus non-marine components. As such, the discussion and interpretations herein focus on trends observed in the bulk carbon isotope record, and comments cannot be made on the isotopic behaviour within the individual carbon isotope reservoirs.

The FCD1 section is the most complete of the four sections detailed in this study (Fig. 3). The $\delta^{13}C_{org}$ profile shows little variation from the base of the Leslei Zone, with values fluctuating continuously between a limited range of -24 to -26 ‰ (averaging ~ -25.7 ‰). Additionally, TOC concentration is consistently low (averaging ~0.5 wt. %) with limited variation. The FCD2 section, which corresponds to the base of the Carinatum Zone to the base of the Harbledownense Zone, exhibits comparable $\delta^{13}C_{org}$ and TOC profiles, with the exception of intermittently dispersed TOC values of ~1-2.8 wt. % (Fig. 5). Such low TOC values for both sections demonstrate that the extent of organic carbon burial at Five Card Draw was minimal, and further, that water-column stagnation and water-column anoxia are unlikely to have been a factor here (*cf*. Jenkyns and Weedon, 2013). Some fluctuation may have been noted in the dataset if both marine and non-marine components of the bulk organic matter had been analysed. However, the relative continuity of the bulk $\delta^{13}C_{org}$ values indicates that overall the bulk organic carbon reservoir at Five Card Draw remained consistent and undisturbed during this part of the Sinemurian.

Some subtle shifts in the $\delta^{13}C_{org}$ and TOC profiles are observed in the LC1 section (base of the Leslei Zone; Fig. 6). The $\delta^{13}C_{org}$ values at LC1 average ~ -25 ‰ over the 20 m section, and show a subtle negative shift to ~ -23 ‰ at approximately 14 m. This is followed, stratigraphically, by an increase in TOC concentration at ~16 m (to ~3 wt. %). Otherwise, TOC levels remain consistently low (< 1 wt. %) for the duration of this section.

Conversely, marked shifts in $\delta^{13}C_{org}$ values are exhibited at LC2 (upper part of the Leslei Zone; Fig. 6). Notably, a gradual positive shift in the carbon isotope profile occurs from 0-29 m in the section (from ~ -26.8 to -23.7 ‰); possibly driven by increased levels of primary productivity (Jenkyns and Weedon, 2013). This is punctuated by an abrupt negative carbon isotope excursion (CIE) at ~ 30 m where values return to ~ -26.8 ‰ (Fig.

6). The $\delta^{13}C_{org}$ profile then recovers abruptly to values of ~ -23.9 ‰. As discussed later, negative $\delta^{13}C_{org}$ excursions observed in organic-rich marine sediments are caused by increased input of ^{12}C into the oceanic-atmospheric reservoir, and can be driven by a number of factors including: volcanogenic CO_2 emissions, dissociation of gas hydrates and upwelling of ^{12}C-enriched bottom-waters.

As in the Five Card Draw section, TOC concentrations for LC1 and LC2 are low (mostly < 2 wt. %), indicating minimal levels of organic carbon burial and preservation. Again, this suggests that the depositional environment in this part of the Panthalassa Ocean was neither stagnant nor anoxic at this time.

However, the gradual positive CIE and abrupt negative CIE are restricted to the upper part of the Leslei Zone at Last Creek. There is no biochronologic or sedimentary evidence to suggest that this interval is missing at Five Card Draw. This suggests that the driving mechanisms for these isotopic shifts were either only present in this specific intra-ocean setting of Panthalassa, or that they were just not recorded in the shallower marginal setting at Five Card Draw. To investigate this further, it is critical that we understand the environments in which these sections were deposited. In addition, comparison with coeval datasets from other global locations will allow us to evaluate whether the signal at Last Creek was influenced by a widespread, potentially global causal mechanism.

7.2 Comparing Five Card Draw to Last Creek: Restricted vs. open-ocean?

Determining the depositional Os isotope composition of marine sediments (initial Os, expressed as $^{187}Os/^{188}Os_{(i)}$) can yield important information regarding the ocean chemistry at the time of deposition. In turn, evaluation of variations in ocean chemistry can provide the key to enhancing our understanding of the depositional environment. The Os isotope composition ($^{187}Os/^{188}Os$) of seawater can be directly controlled by three major inputs: (1) radiogenic input from weathering of continental crust ($^{187}Os/^{188}Os$ of ~1.4; Peucker-Ehrenbrink and Jahn, 2001); (2) unradiogenic contribution from meteorites ($^{187}Os/^{188}Os$ of ~0.12; Ravizza and Peucker-Ehrenbrink, 2003); (3) an unradiogenic signal from a mantle-derived source ($^{187}Os/^{188}Os$ of ~0.12; Allègre and Luck, 1980; Esser and Turekian, 1993; Sharma *et al.,* 1997; Levasseur *et al.,* 1998; Peucker-Ehrenbrink and Ravizza, 2000).

The present-day seawater Os isotope composition may be relatively uniform ($^{187}Os/^{188}Os$ ratio of ~1.06; Levasseur *et al.,* 1998; Peucker-Ehrenbrink and Ravizza, 2000) but it has varied significantly throughout geological time. The short seawater residence time of Os of ~10-40 Ka (Sharma *et al.,* 1997; Oxburgh, 1998; Levasseur *et al.,* 1998; Peucker-Ehrenbrink and Ravizza, 2000), longer than the mixing time of the oceans (~2 – 4 Ka; Palmer *et al.,* 1988), allows the Os isotope composition to respond rapidly to any alterations in the composition and flux of these inputs (Oxburgh, 1998; Cohen *et al.,* 1999). This has been successfully exploited by past studies, where Os has been used as a chemostratigraphic marker of significant volcanic events (Cohen *et al.,* 1999; Ravizza and Peucker-Ehrenbrink, 2003).

In order to look critically at the Os data herein there needs to be an understanding of the background seawater Os isotope composition at this time. However, currently no studies conclusively document background seawater Os for the Early Jurassic. The first estimation of stable, steady-state $^{187}Os/^{188}Os$ values for the Sinemurian is given as ~ 0.47 (Kuroda *et al.,* 2010). The sampled section (Triassic-Jurassic chert succession from Kurusu, Japan; Kuroda *et al.,* 2010) was positioned to the east of the separating supercontinent, in an intra-ocean setting. The recorded Os isotope composition would have likely been less directly affected by nearby continental flux, and potentially may be a good representation of open ocean chemistry at this time. For this investigation, we will assume that this value represents the best estimation of background seawater Os isotope composition during the Early Jurassic.

The $^{187}Os/^{188}Os_{(i)}$ values from Last Creek (LC1 and LC2) fluctuate steadily between ~0.11-0.91 (Table 1; Fig. 6). Of the 17 samples, 9 have $^{187}Os/^{188}Os_{(i)}$ values of

<0.30, indicating an unradiogenic Os flux into the water column. Whilst the sampling interval is relatively low resolution, it is likely that these values result from a juvenile, mantle-derived flux rather than an extraterrestrially-derived source, based upon the shape of the Os isotope profile. Following a meteorite impact, such as that at Cretaceous-Paleogene boundary, the Os isotope profile will suddenly shift to unradiogenic $^{187}Os/^{188}Os$ values, before a gradual recovery to steady-state values over ~200 Ka (Ravizza and Peucker-Ehrenbrink, 2003). Although the extraterrestrial flux to Earth during the Jurassic is poorly constrained, there is currently no evidence external to this study that supports a meteorite impact event at this time. Rather, an open-ocean arc depositional setting with an intermittent flux of unradiogenic Os is more likely to explain the $^{187}Os/^{188}Os_{(i)}$ values observed at Last Creek.

The Os isotope composition of samples from ~40 m of the upper part of the Leslei Zone at Five Card Draw, ranges from ~0.20-2.81 (Table 1, Fig. 5). However, of these samples (n=11), only 1 has an Os isotope composition that can be interpreted as unradiogenic (~0.20). Further, and in contrast to Last Creek (Fig. 7), 7 have radiogenic $^{187}Os/^{188}Os_{(i)}$ values that are greater than the average documented $^{187}Os/^{188}Os_{(i)}$ value for continental crust (~1.4; Peucker-Ehrenbrink and Jahn, 2001). This indicates that there was a significant contribution of continental material, likely highly evolved and rich in radiogenic Os, into the water column at Five Card Draw during this time. A number of possible sources, known to have high concentrations of Re and therefore radiogenic Os, may have eroded into the water column to produce the observed radiogenic Os isotope signal, including: (1) old and highly evolved continental crust; (2) black shales; and (3) a mineral deposit (sulphide-rich).

Five Card Draw is known to have been deposited in a continental margin setting, and so the presence of an erosional continental component in these samples should be expected. However, the presence of such highly radiogenic Os isotope values strongly indicates that, as well as the occurrence of persistent continental inundation in this area, free circulation with the open ocean at this time in the Sinemurian was not occurring. This can be further supported by comparing the Last Creek (open-ocean signal) and Five Card Draw datasets (Fig. 7). This study therefore suggests that deposition at Five Card Draw occurred in a partially restricted basin on the continental margin. Such a marked contrast between the depositional settings of these two field sites (Nevada and an allocthonous terrane) is also noted in a preliminary global Neodymium dataset assembled by Dera et al. (in press).

Furthermore, early mapping of the Triassic rocks adjacent to the Pamlico-Luning lithotectonic assemblage showed facies distributions suggesting a partially enclosed embayment on the western margin of the continent (Ferguson and Muller, 1949). The basin, named the 'Luning Embayment' by Ferguson and Muller (1949), was the depositional setting for the Volcano Peak Group which includes the Sunrise Formation (Taylor et al., 1983; Taylor and Smith, 1992).

7.3 A global carbon isotope excursion at Last Creek?

To gain a global perspective on fluctuations within the carbon reservoir during the Sinemurian, it is necessary to compare coeval data from ocean basins that are: 1) geographically far-removed and 2) contain sediments from various depositional settings. As has been described, carbon-isotope data from western North America was compiled from two areas of the northeast Panthalassa that represent sedimentary deposition in an open-ocean environment (Last Creek) and in a restricted basin setting (Five Card Draw). These datasets were then compared with those previously established for the epicontinental seaway of northwest Europe (Fig. 8).

In the European dataset, there is a large gradual ~4 ‰ positive $\delta^{13}C$ excursion throughout the Turneri Zone, where values reach ~ –24 ‰ in the upper part of the zone before showing a gradual return to more negative values of ~ –28 ‰ in the Obtusum Zone (Fig. 8; Jenkyns and Weedon, 2013). Jenkyns and Weedon (2013) note that this positive excursion does not co-occur with an elevated concentration of organic carbon in the upper part of the Turneri Zone and therefore cannot be attributed to local patterns of organic-matter burial (such as water column deoxygenation). Rather they point to a long-term change in seawater isotope chemistry to explain the positive excursion. In support of this, Van de Schootbrugge et al. (2005) and Schwab and Spangenber (2007) also note a similar positive peak in $\delta^{13}C$ records during the Turneri Zone in the Tethyan domain. In addition, Jenkyns and Weedon (2013) highlight a prominent negative excursion at the Obtusum-Oxynotum boundary (which is equivalent to the Carinatum-Harbledownense boundary at FCD2), that they have attributed to palaeoclimatic and faunal changes (Fig. 8).

In western North America, a pronounced positive excursion of similar magnitude and duration is recognized at the Last Creek locality (blue line in Fig. 8). As with the European data, this positive carbon-isotope excursion from the un-restricted northeast Panthalassa does not co-occur with elevated organic carbon burial (Fig. 6). However, our data differs in that there is a large (and abrupt) negative shift of ~ 3 ‰ in the uppermost Leslei Zone which seems to interrupt the pronounced gradual positive excursion. During this abrupt negative CIE, values reach ~ –27 ‰ for ~ 4 m in the section. Curiously, as previously discussed, this pattern is not evident in the coeval succession at Five Card Draw (green and red lines in Fig. 8). Throughout the upper part of the Leslei Zone, carbon-isotope values predominantly range between –25 ‰ and –26 ‰ and do not show any positive or negative trend. Similarly there is also no indication of elevated organic carbon burial throughout this interval. Further, $\delta^{13}C_{org}$ values at Five Card Draw 2 show a subtle positive increase (~ 1 ‰) throughout the duration of Carinatum Zone, in contrast to the abrupt negative excursion seen in Europe at the Obtusum-Oxynotum interval (Jenkyns and Weedon, 2013).

The distinct similarities between the positive CIE in the upper part of the Leslei Zone (approximately equivalent to the Turneri Zone) observed in the Last Creek and Dorset sections, suggest that these sites likely record a widespread and potentially global carbon isotope signal. The lack of comparable signals at Five Card Draw indicates, however, that this signal may only have been recorded in open-ocean or unrestricted marine environments, and in turn, that basinal restriction may hide global carbon cycle records. As with the conclusions of Jenkyns and Weedon (2013), the event in western North America is not correlative with significant organic carbon enrichment and therefore was not controlled by local basin stagnation and water column deoxygenation. Rather, a more-likely explanation might involve increased and widespread primary productivity that may be associated with eustatic sea level rise (noted in Donovan et al., 1979; Jenkyns and Weedon, 2013). Further, heightened inundation of continental material into the basin at Five Card Draw may have played a key role in supressing a carbon isotope signal induced by such increased levels of primary productivity.

The positive CIE interval in Panthalassa is interrupted by an abrupt negative CIE that only seems to occur in the Last Creek section. In the geological record, negative CIEs are thought to record the injection of isotopically light carbon (^{12}C) into the oceanic-atmospheric reservoirs by a number of sources that include: upwelling of ^{12}C-rich bottom water (ocean reservoir only) (Küspert, 1982; Jenkyns, 1988; McArthur et al., 2008), dissociation of gas hydrates ($\delta^{13}C$ = ~ –60 ‰, Hesselbo et al., 2000), volcanogenic CO_2 emissions ($\delta^{13}C_{CO2}$ between –5 ‰ and –25 ‰, Deines, 2002) and oxidation of organic matter on exposed shelf sediments during eustatic sea level fall (Jenkyns et al., 2002 and references therein). In relation to these potential sources, the abrupt negative CIE in the upper part of the Leslei Zone: 1) does not occur in multiple localities, implying that it is being driven locally; 2) does not contain $\delta^{13}C$ values that are indicative of methane gas release (e.g. > –30 ‰ in Hesselbo et al., 2000), assuming that any methane added to the reservoir would be present in recognisable amounts; and 3) occurs during a time of eustatic sea level rise and therefore could not be caused by the oxidation of organic matter during regressive cycles. This study therefore suggests that the negative CIE observed only at Last Creek may have been driven by localised bottom-water upwelling during the sea-level rise.

8. Conclusions

Investigation of two field sites from western North America has yielded a number of important conclusions regarding Sinemurian depositional environments and ocean chemistry:

1. Although bulk TOC profiles for Five Card Draw (Nevada) and Last Creek (British Columbia) are comparable, bulk carbon isotope profiles at Last Creek show significant variation, in contrast to those at Five Card Draw.
2. Osmium isotope analysis demonstrates that the successions at Five Card Draw and Last Creek were deposited in contrasting environments (partially restricted vs. open-ocean).
3. The gradual positive CIE observed at LC2 corresponds to a coeval positive CIE of similar duration in Dorset, UK (Jenkyns and Weedon, 2013), and additional Tethyan domains (Schootbrugge et al., 2005; Schwab and Spangenberg, 2007) suggesting that this is a globally controlled CIE. A likely causal factor may have been a widespread increase in primary productivity.
4. Although present on a potentially global scale, this positive CIE is not observed at Five Card Draw. Deposition in a partially restricted basin, combined with significant continental inundation, is likely to be the reason for this.
5. An abrupt negative CIE is observed at LC2 but is not present at Five Card Draw nor in the European section, suggesting that this CIE was driven by mechanisms local to this specific field site. The most likely cause is upwelling of ^{12}C-rich bottom-waters.

Figure captions

Fig. 3. Stratigraphic columns for the Five Card Draw (FCD1 and FCD2) and Last Creek (LC1 and LC2) sections, showing the stratigraphic and lateral relationship of the 4 sections to one another.

Fig. 1. Maps showing the location of: A) the study areas in North America; B) Five Card Draw in Nevada, USA; C) the Five Card Draw sampling areas; D) Last Creek in British Columbia, Canada; E) the Last Creek sampling sites. B and C modified from Taylor et al. (1983). D and E modified from Macchioni et al. (2006).

Fig. 2. Early Jurassic palaeogeographic map showing positions of the sampling areas discussed in this study. Solid black stars indicate the position of Five Card Draw, USA (western continental margin of North America) and Last Creek, Canada (eastern Panthalassa, open-ocean setting). Hollow star denotes position of the Dorset, UK site (Jenkyns and Weedon, 2013). Map modified from www.scotese.com.

Fig. 4. Correlation of the Sinemurian ammonite zonation of western North America with northwest Europe by Taylor *et al*. (2001 modified by Longridge, *et al.*, 2006). Ranges of ammonite genera collected during this study are shown in column 2. Ages of stage boundaries and uncertainties are from Gradstein *et al*. (2012); the age of the equivalent of the basal Obtusum Zone is from Pálfy *et al*. (2000).

Fig. 5. Total Organic Carbon, $\delta^{13}C_{org}$, and Re-Os isotope profiles for FCD1 and FCD2.

Fig. 6. Total Organic Carbon, $\delta^{13}C_{org}$, and Re-Os isotope profiles for LC1 and LC2.

Fig. 7. Plot comparing the initial $^{187}Os/^{188}Os$ values for FCD1 (blue squares), LC1 (solid red squares) and LC2 (hollow red squares). The transparent blue box indicates 1 standard deviation either side of the average $^{187}Os/^{188}Os_{(I)}$ value for FCD1 (1.6), and the red box indicates 1 standard deviation either side of the average $^{187}Os/^{188}Os_{(I)}$ value for LC1 and LC2 (0.36). Dashed lines indicate $^{187}Os/^{188}Os$ threshold values: 1. Average mantle value (0.12); 2. Estimation of Early Jurassic steady-state seawater $^{187}Os/^{188}Os$ value (0.47) taken from Kuroda et al. (2010); and 3. Average value of continental crust (1.4).

Fig. 8. Figure comparing $\delta^{13}C_{org}$ data from western North America (Five Card Draw and Last Creek; this study) with a coeval $\delta^{13}C_{org}$ dataset from Europe (Dorset, UK; Jenkyns and Weedon, 2013). Yellow box marks positive CIE observed in western North America and UK. Orange box shows negative CIE observed at Last Creek (blue line). Green, red and blue lines denote FCD1, FCD2 and LC1 & 2 sections, respectively. Biostratigraphy is given to demonstrate correlation of Sinemurian zonation in North America and Europe.

Table 1. Re-Os isotope data for Five Card Draw (FCD1) and Last Creek (LC1 and LC2).

Acknowledgements

Thanks to Steve Calvert and Maureen Soon (UBC) for use of their facility during the sample preparation stage. Paul Smith acknowledges support of the Natural Sciences and Engineering Research Council of Canada (grant 8493). The isotopic component of this study was partially funded by a NERC grant to Darren Gröcke (NE/H021868/1). We would also like to thank the editor, J. B. Riding and two anonymous reviewers for their constructive comments.

References

Allègre, C. J., Luck, J.-M., 1980. Osmium isotopes as petrogenetic and geological tracers. Earth Planet. Sci. Lett. 48, 148-154.

Cariou, E., Hantzpergue, P. (coord. Groupe Français d'Étude du Jurassique), 1997. Biostratigraphie du Jurassique Quest-Européen et méditerranéen: zonations paralléles et distribution des invertébrés et microfossiles. Bull. Cent. Rech. Elf Explor. Prod., Mémoir.17, 1-440.

Caruthers, A. H., Gröcke, D. R, Smith, P. L., 2011. Global carbon isotope excursion during the Toarcian Oceanic Anoxic Event. Earth Planet. Sci. Lett., 307, 19-26

Cohen, A. S., Coe, A. L., 2007. The impact of the Central Atlantic Magmatic Province on climate and on the Sr- and Os-isotope evolution of seawater. Palaeogeogr. Palaeoclimatol. Palaeoecol. 244, 374-390.

Cohen, A. S., Coe, A. L., Bartlett, J. M., Hawkesworth, C. J., 1999. Precise Re-Os ages of organic-rich mudrocks and the Os isotope composition of Jurassic seawater. Earth Planet. Sci. Lett. 167, 159-173.

Creaser, R. A., Papanastassiou, D. A., Wasserburg, G. J., 1991. Negative thermal ion mass spectrometry of osmium, rhenium and iridium. Geochim. Cosmochim. Acta. 55, 397-401.

Cumming, V. M., Poulton, S. W., Rooney, A. D., Selby, D., 2013. Anoxia in the terrestrial environment during the late Mesoproterozoic. Geology. 41 (5), 583-586.

Dean, W. T., Donovan, D. T., Howarth, M. K., 1961. The Liassic ammonite zones and subzones of the north-west European province. Bull. British Museum (Natural History). 4 (10), 438-505.

Deines, P., 2002. The carbon isotope geochemistry of mantle xenoliths. Earth-Sci. Rev. 58, 247–278.

Dera, G., Prunier, J., Smith, P. L, Haggart, J., Popov, E., Guzhov, A., Rogov, M., Delsate, D., Thies, D., Cuny, G., Pucéat, E., Charbonnier, G., Bayon, G., In press. Nd isotope constraints on ocean circulation, paleoclimate, and continental drainage during the Jurassic breakup of Pangea. Gondwana Research.

Donovan, D. T., Horton, A., Ivimey-Cook, H. C., 1979. The transgression of the Lower Lias over the northern flank of the London Platform. J. Geol. Soc. London. 136, 165–173.

Esser, B. K., Turekian, K. K., 1993. The osmium isotopic composition of the continental crust. Geochim. Cosmochim. Ac. 57, 3093-3104.

Ferguson, H. G., Muller, S. W., 1949. Structural geology of the Hawthorne and Tonopah quadrangles, Nevada. U. S. Geol. Surv. Prof. Pap. 216, 1-53.

Gradstein, F. M., Ogg, J. G., Schmitz, M. D., Ogg, G. M. (eds), 2012. The Geologic Time Scale 2012. Elsevier BV, Oxford, UK; Amsterdam, The Netherlands; Waltham, USA. 1-793.

Hallam, A., 1981. A revised sea-level curve for the Early Jurassic. J. Geol. Soc. London. 138, 735-743.

Hesselbo, S.P., Gröcke, D.R., Jenkyns, H.C., Bjerrum, C.J., Farrimond, P., Morgans Bell, H.S., Green, O.R., 2000. Massive dissociation of gas hydrate during a Jurassic oceanic anoxic event. Nature. 406, 392–395.

Hesselbo, S. P., Jenkyns, H. C., Duarte, L.V., Oliveira, L. C.V., 2007. Carbon-isotope record of the Early Jurassic (Toarcian) Oceanic Anoxic Event from fossil wood and marine carbonate (Lusitanian Basin, Portugal). Earth Planet. Sci. Lett. 253, 455–470.

Jenkyns, H.C., 1988. The Early Toarcian (Jurassic) event: stratigraphy, sedimentary and geochemical evidence. Am. J. Sci. 288, 101–151.

Jenkyns, H. C., Jones, C. E., Gröcke, D. R., Hesselbo, S. P., Parkinson, D. N., 2002. Chemostratigraphy of the Jurassic System: applications, limitations and implications for palaeoceanography. J. Geol. Soc. London. 159, 351–378.

Jenkyns, H. C., 2010. Geochemistry of oceanic anoxic events. Geochem. Geophy. Geosy. 11 (3). Q03004.

Jenkyns, H. C., Weedon, G. P., 2013. Chemostratigraphy ($CaCO_3$, TOC, $\delta^{13}C_{org}$) of Sinemurian (Lower Jurassic) black shales from the Wessex Basin, Dorset and palaeoenvironmental implications. Newsl. Stratigr. 46 (1), 1-21.

Korte, C., Hesselbo, S. P., 2011. Shallow marine carbon and oxygen isotope and elemental records indicate icehouse-greenhouse cycles during the Early Jurassic. Paleoceanography. 26, PA4219, doi: 10.1029/2011PA002160.

Kuroda, J., Hori, R. S., Suzuki, K., Gröcke, D. R., Ohkouchi, N., 2010. Marine osmium isotope record across the Triassic-Jurassic boundary from a Pacific pelagic site. Geology. 38, 1095-1098.

Küspert, W., 1982. Environmental changes during oil shale deposition as deduced from stable isotope ratios, in: Einsele, G., and Seilacher, A. (Eds.), Cyclic and Event Stratification. Springer, Berlin, 482–501.

Levasseur, S., Birck, J.-L., Allègre, C. J., 1998. Direct Measurement of Femtomoles of Osmium and the $^{187}Os/^{186}Os$ Ratio in Seawater. Science. 282, 272-274.

Longridge, L. M., Smith, P. L., Tipper, H. W., 2006. The Early Jurassic ammonite *Badouxia* from British Columbia, Canada. Palaeontology. 49(4), 795-816.

McArthur, J. M., Algeo, T. J., van de Schootbrugge, B., Li, Q., Howarth, R.J., 2008. Basinal restriction, black shales, Re-Os dating, and the Early Toarcian (Jurassic) oceanic anoxic event. Paleoceanography, 23, 1–22.

Macchioni, F., Smith, P. L., Tipper, H. W., 2006. Late Early Sinemurian (Early Jurassic) ammonites from the Taseko Lakes map area, British Columbia. Palaeontology. 49(3), 557-583.

Meister, C., Blau, J., Schlatter, R., Schmidt-effing, R., 2002. Ammonites from the Lower Jurassic (Sinemurian) of Tenango De Doria (Sierra Madre Oriental, Mexico). Part II: Phylloceratoidea, Lytoceratoidea, Schlotheimiidae, Arietitinae, Oxynoticeratidae, and Eoderoceratidae. Revue Paléobiol., 21 (1), 391-409.

Oldow, J. S., 1978. Triassic Pamlico Formation; an allochthonous sequence of volcanogenic-carbonate rocks in west-central Nevada. *In:* Howell, D. G. and McDougall, K. A. (eds). Mesozoic palaeogeography of the western United States. Society of Economic Palaeontologists and Mineralogists, Pacific Coast Palaeogeography Symposium. 2, 253-270.

Monger, J. W. H., 2011. An overview of the tectonic history of the southern Coast Mountains, British Columbia. In Haggart, J. W. and Smith, P.L. (Eds). Canadian Paleontology Conference, Field Trip Guidebook No 16. Geological Association of Canada, Paleontology Division, 1-11.

Oxburgh, R., 1998. Variations in the osmium isotope composition of sea water over the past 200,000 years. Earth Planet. Sci. Lett.. 159, 183-191.

Page, K. N., 2003. The Lower Jurassic of Europe: its subdivision and correlation. Geol. Surv. Denmark and Greenland Bull. 1, 23-59.

Pálfy, J., Smith, P. L., Tipper, H. W., 1994. Sinemurian (Lower Jurassic) ammonoid biostratigraphy of the Queen Charlotte Islands, Western Canada. Geobios. 27, 385-393.

Pálfy, J., Smith, P. L., Mortensen, J. K., 2000. A U-Pb and $^{40}Ar/^{39}Ar$ time scale for the Jurassic. Can. J. Earth Sci. 37, 923-944.

Palmer, M. R., Falkner, K. K., Turekian, K. K., Calvert, S. E., 1988. Sources of osmium isotopes in manganese nodules. Geochim. Cosmochim. Ac. 52, 1197-1202.

Peucker-Ehrenbrink, B., Jahn, B., 2001. Rhenium-osmium isotope systematics and platinum group element concentrations: Loess and the upper continental crust. Geochem. Geophy. Geosy. 2, 1061-1083.

Peucker-Ehrenbrink, B., Ravizza, G., 2000. The marine osmium isotope record. Terra Nova. 12, 205-219.

Porter, S. J., Selby, D., Suzuki, K., Gröcke, D., 2013. Opening of a trans-Pangaean marine corridor during the Early Jurassic: Insights from osmium isotopes across the Sinemurian-Pliensbachian GSSP, Robin Hood's Bay, UK. Palaeogeogr. Palaeoclimatol. Palaeoecol. 375, 50-58.

Ravizza, G., Peucker-Ehrenbrink, B., 2003. Chemostratigraphic Evidence of Deccan Volcanism from the Marine Osmium Isotope Record. Science. 302, 1392-1395.

Riding, J. B., Leng, M. J., Kender, S., Hesselbo, S. P., Feist-Burkhardt, S., 2013. Isotopic and palynological evidence for a new Early Jurassic environmental perturbation. Palaeogeogr. Palaeoclimatol. Palaeoecol. 374, 16-27.

Schiarizza, P., Gaba, R. G., Glover, J. K., Garver, J. I., Umhoefer, P. J., 1997. Geology and mineral occurrences of the Taseko Bridge River Area. B. C. Geol. Surv. Bull. 100, 1-10.

Schwab, V. F., Spangenberg, J. E., 2007. Molecular and isotopic characterization of biomarkers in the Frick Swiss Jura sediments: A palaeoenvironmental reconstruction on the northern Tethys margin. Org. Geochem. 38, 419-439.

Selby, D., Creaser, R. A., 2003. Re-Os geochronology of organic rich sediments: an evaluation of organic matter analysis methods. Chem. Geol. 200, 225-240.

Sharma, M., Papanastassiou, D. A., Wasserburg, G. J., 1997. The concentration and isotopic composition of osmium in the oceans. Geochim. Cosmochim. Ac. 61, 3287-3299.

Silberling, J., 1959. Pre-Tertiary stratigraphy and Upper Triassic palaeontology of the Union District, Shoshone Mountains, Nevada. U. S. Geol. Surv. Prof. Paper 322, 1-67.

Smith, P. L., Monger, J. W. H., Arthur, A., Poulton, T. P., Tipper, H. W., 1998. Southwestern British Columbia. In Smith, P.L. (Ed.) A Field Guide for the Fifth International Symposium on the Jurassic System, Vancouver. International Union of Geological Sciences, 230-307.

Smith, P. L., Tipper, H. W., 2000. The schlotheimiid succession across the Hettangian-Sinemurian boundary (Lower Jurassic), Taseko Lakes map area, British Columbia, Canada. Rev. Paléobiologie, Genève, Volume Spécial 8. 1-12.

Speed. R. C, 1979. Collided Palaeozoic Microplate in the Western United States. J. Geol. 87 (3). 279-292.

Taylor, D. G., Guex, J., Rakus, M., 2001. Hettangian and Sinemurian ammonoid zonation for the Western Cordillera of North America. Bull. Société vaudoise Sci. Nat. 87 (4), 381-421.

Taylor, D. G., Smith, P. L., 1992. Nevada. *In*: Westermann, G. E. G. (Ed.). The Jurassic of the Circum-Pacific. Camb. Univ. Press. 77-83.

Taylor, D. G., Smith, P. L., Laws, R. A., Guex, J., 1983. The stratigraphy and biofacies trends of the Lower Mesozoic Gabbs and Sunrise formations, west-central Nevada. Can. J. Earth Sci. 20, 1598-1608.

Umhoefer, P. J., Tipper, H. W., 1998. Stratigraphy, depositional environment and tectonic setting of the Upper Triassic to Middle Jurassic rocks of the Chilcotin Ranges, southwestern. B. C. Geol. Surv. Can. Bull. 519, 1-58.

Van de Schootbrugge, B., Bailey, T. R., Rosenthal, Y., Katz, M. E., Wright, J. D., Miller, K. G., Feist-Burkhardt, S., Falkowski, P. G., 2005. Early Jurassic climate change and the radiation of organic-walled phytoplankton in the Tethys Ocean. Paleobiology. 31 (1), 73-97.

Völkening, J., Walczyk, T., Heumann, K. G. 1991. Osmium isotope ration determinations by negative thermal ionization mass spectrometry. Int. J. Mass. Spec. Ion. Proc. 105 (2), 147-159.

www.scotese.com (Fig. 2: Pangaean reconstruction in the Sinemurian)

***Highlights (for review)**

New high resolution geochemistry of Lower Jurassic marine sections in western North America: A global positive carbon isotope excursion in the Sinemurian?

Highlights

- New osmium isotope and carbon isotope data for two Early Jurassic marine sections
- Gradual positive CIE in upper Leslei Zone at Last Creek
- Last Creek positive CIE likely reflects a global carbon isotope signature
- Locally driven abrupt negative CIE also observed at Last Creek
- Os isotopes show that both LC and FCD were deposited in contrasting environments

Figure 1

Click here to download Figure: Fig 1 Location maps.pdf

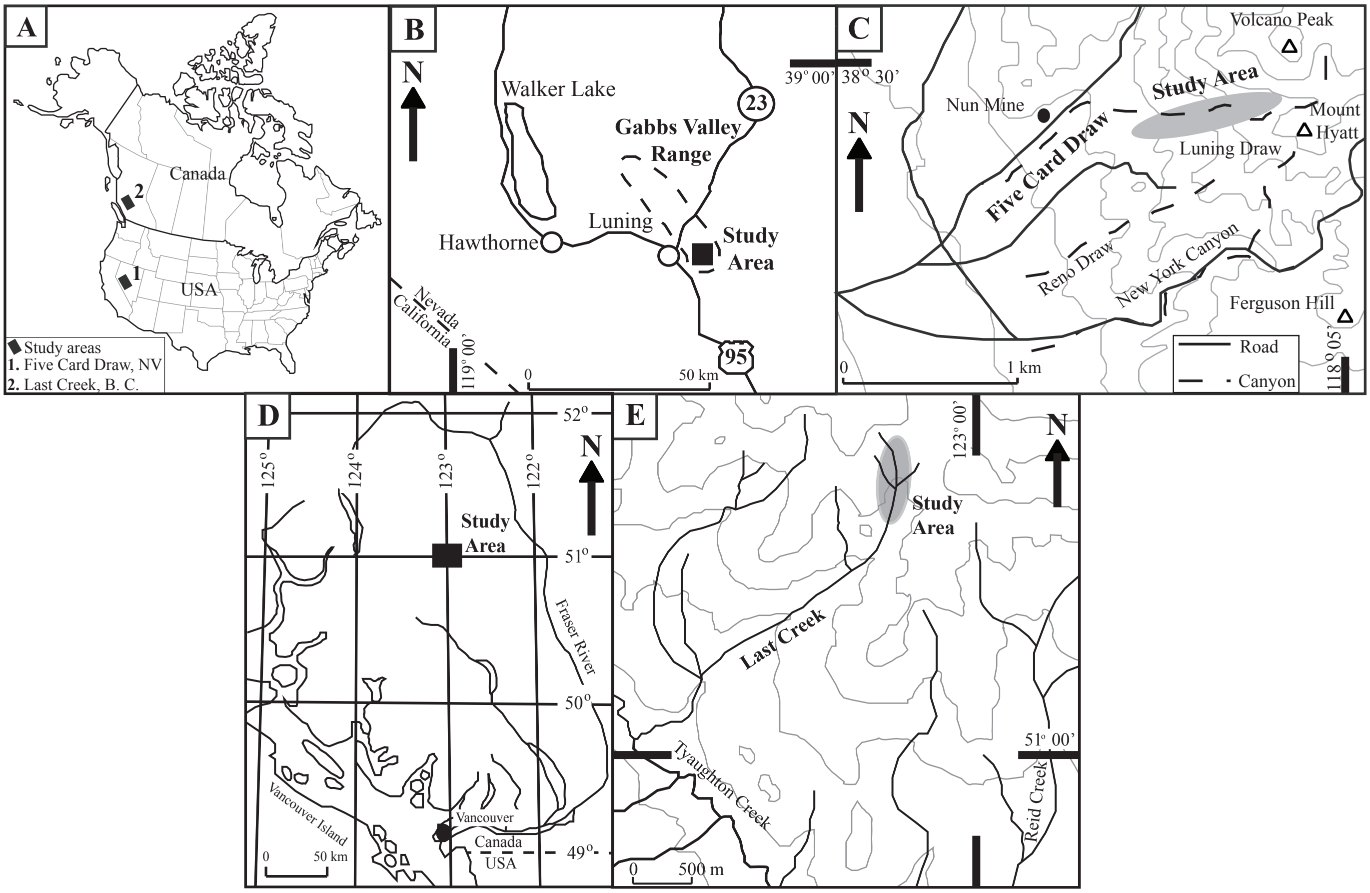

Figure 2

Click here to download Figure: Fig 2 Global Paleogeography bw.pdf

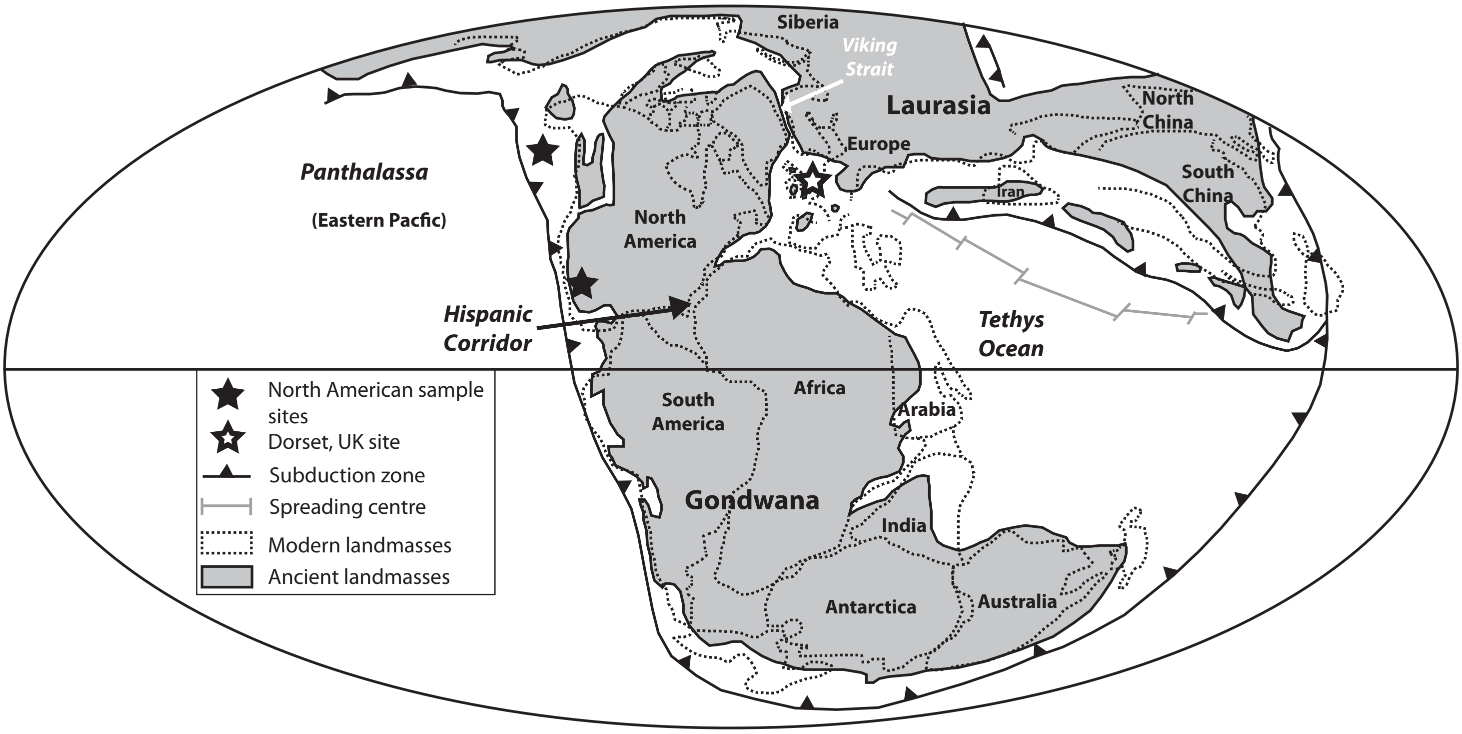

Figure 3

Click here to download Figure: Fig 3 Sinemurian Strat columns.pdf

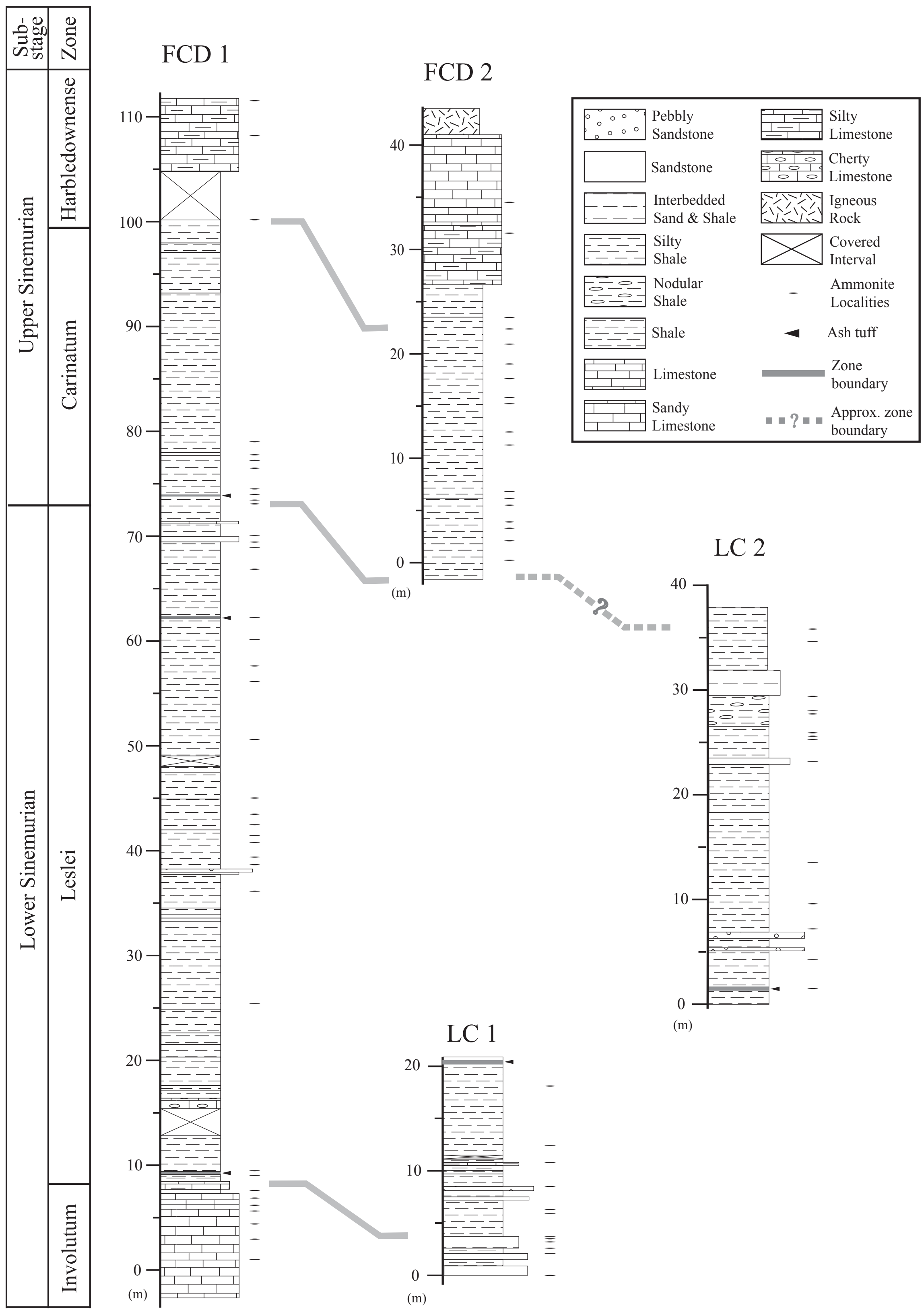

fig_4_biozone_correlation[1].pdf

Click here to download Figure: Fig_4_Biozone_correlation[1].pdf

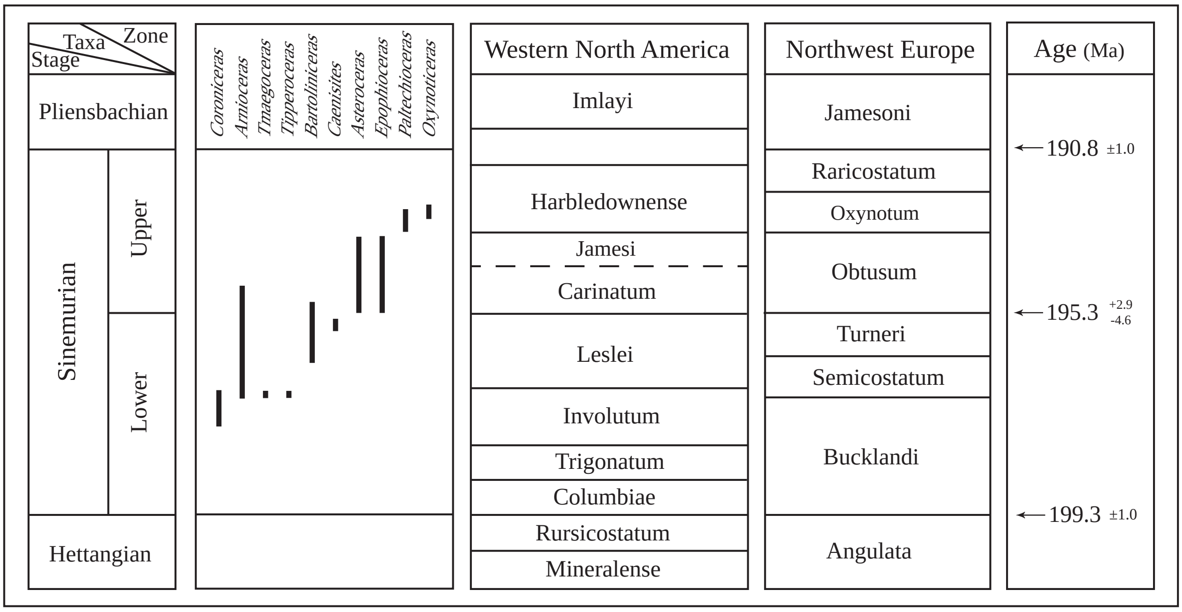

fig_5_fcd_isotope_profiles[1].pdf

Click here to download Figure: Fig_5_FCD_isotope_profiles[1].pdf

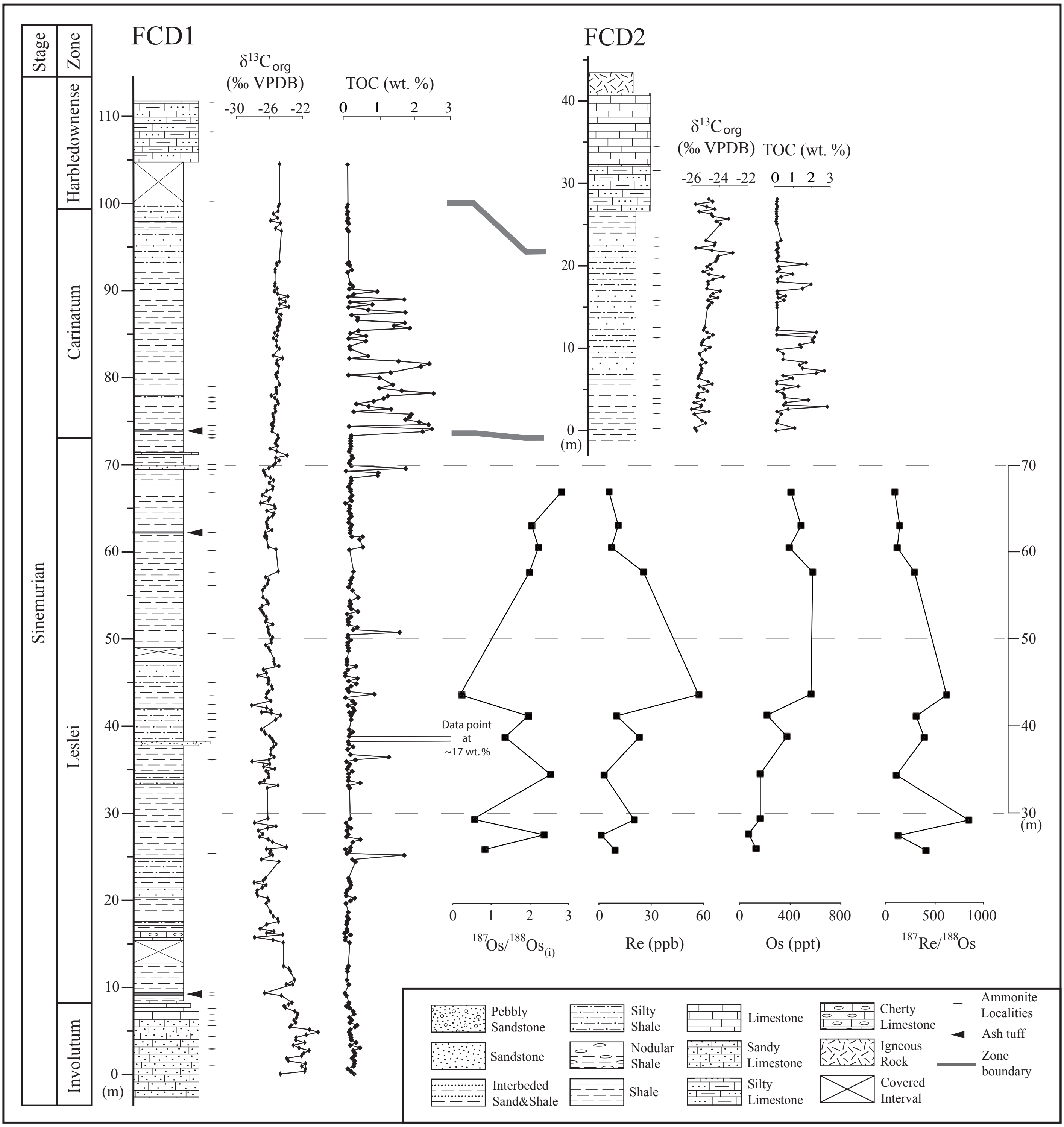

fig_6_lc_isotope_profiles[1].pdf

Click here to download Figure: Fig_6_LC_isotope_profiles[1].pdf

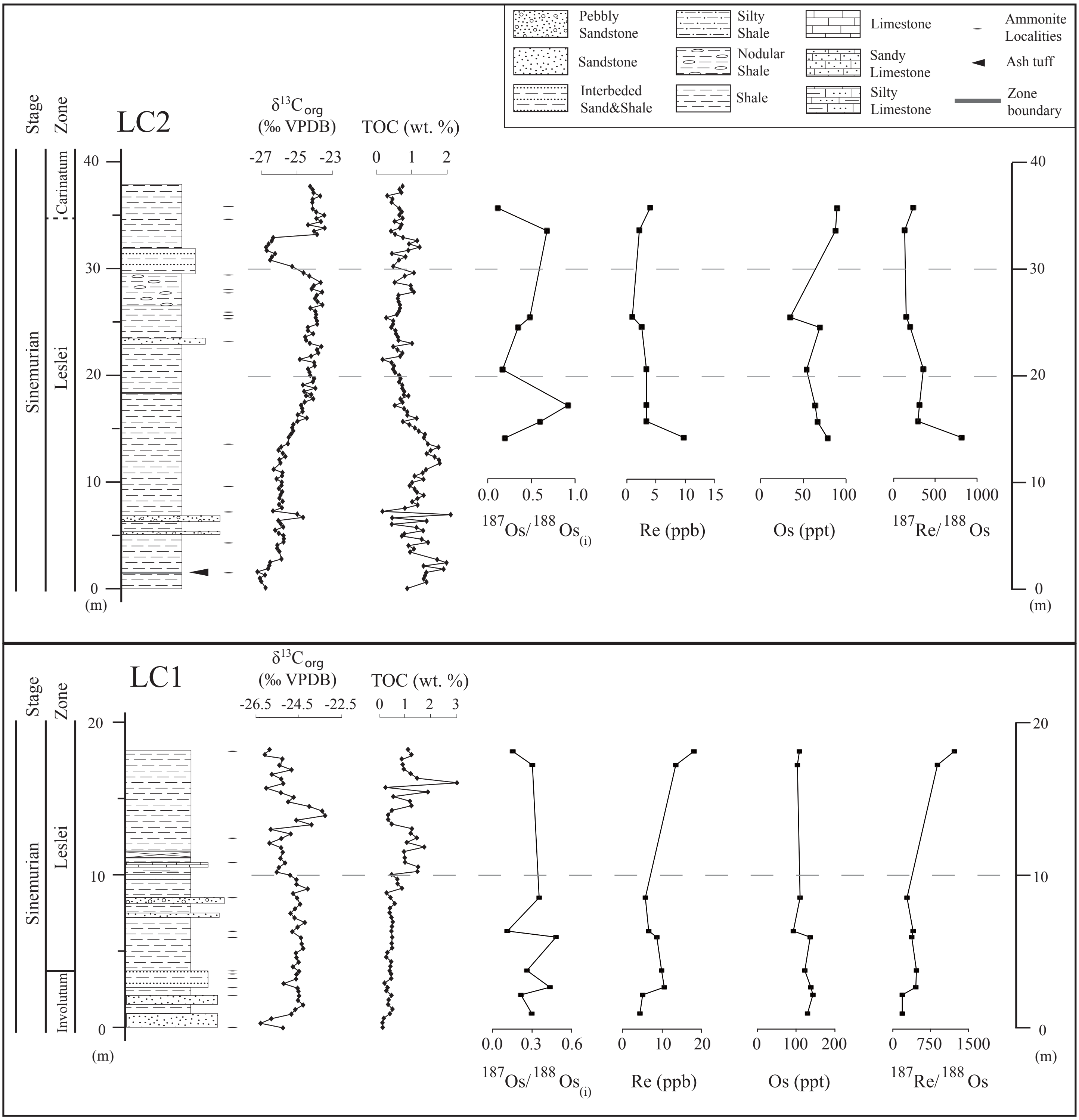

fig_7_os_isotope_data[1].pdf

Click here to download Figure: Fig_7_Os_isotope_data[1].pdf

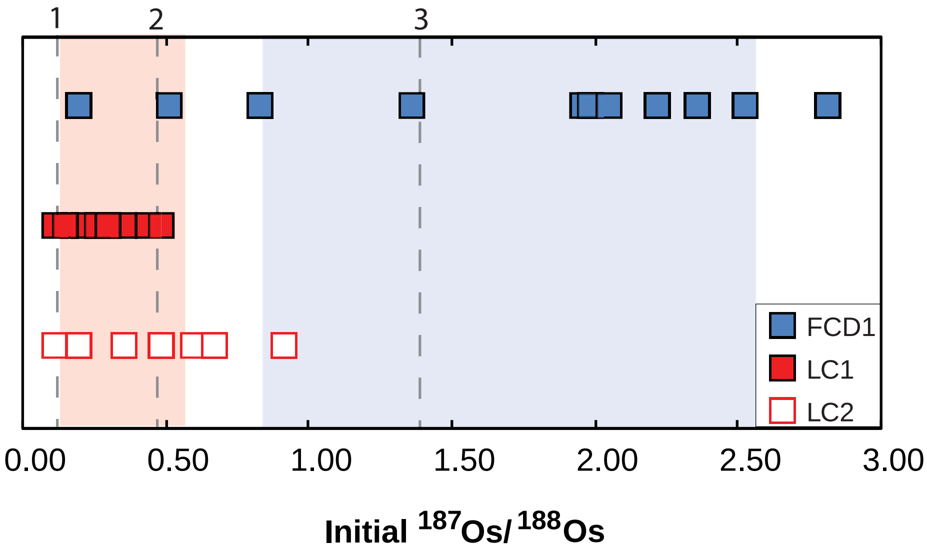

fig_8_all_c_isotope_data[1].pdf
Click here to download Figure: Fig_8_All_C_isotope_data[1].pdf

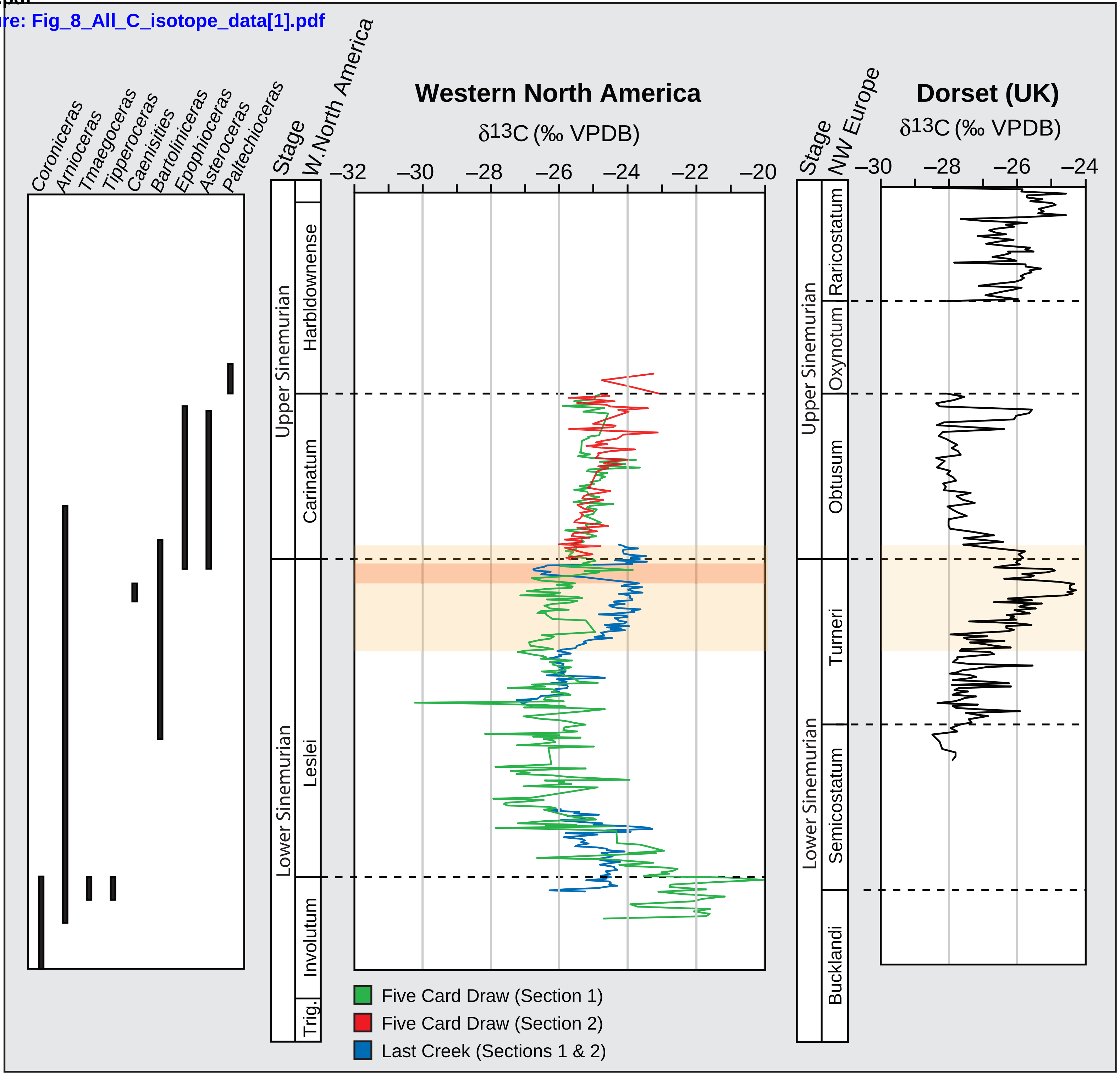

Sample	Re (ppb)	Os (ppt)	$^{187}Re/^{188}Os$	$^{187}Os/^{188}Os$	Rho[a]	$^{187}Os/^{188}Os_{(i)}$
Five Card Draw, Nevada, USA						
FCD1-066	9.1 ± 0.0	134.5 ± 0.8	413.7 ± 3.2	2.177 ± 0.02	0.757	0.83
FCD1-071	1.5 ± 0.0	74.1 ± 0.8	128.9 ± 2.2	2.780 ± 0.05	0.704	2.36
FCD1-076	20.6 ± 0.1	165.1 ± 1.0	845.0 ± 5.5	3.265 ± 0.02	0.778	0.52
FCD1-082	2.9 ± 0.0	167.4 ± 1.6	114.3 ± 1.3	2.899 ± 0.04	0.666	2.53
FCD1-096	23.3 ± 0.1	374.9 ± 1.6	398.5 ± 1.8	2.653 ± 0.01	0.526	1.36
FCD1-101	10.1 ± 0.0	215.3 ± 1.4	309.8 ± 2.1	2.962 ± 0.02	0.673	1.95
FCD1-110	57.1 ± 0.2	566.9 ± 1.9	616.5 ± 2.4	2.203 ± 0.01	0.389	0.20
FCD1-150	25.7 ± 0.1	577.7 ± 2.4	293.2 ± 1.2	2.938 ± 0.01	0.450	1.98
FCD1-152	7.2 ± 0.0	393.0 ± 3.2	117.4 ± 1.1	2.601 ± 0.03	0.653	2.22
FCD1-159	11.3 ± 0.0	483.9 ± 2.7	147.3 ± 0.8	2.526 ± 0.01	0.559	2.05
FCD1-171	5.9 ± 0.0	407.4 ± 2.4	96.7 ± 0.6	3.126 ± 0.02	0.547	2.81
Last Creek, British Columbia, Canada						
LC1-004	4.5 ± 0.0	129.0 ± 1.1	184.4 ± 2.8	0.897 ± 0.02	0.696	0.30
LC1-008	5.2 ± 0.0	143.9 ± 0.9	190.4 ± 1.9	0.833 ± 0.01	0.679	0.21
LC1-010	10.6 ± 0.0	137.8 ± 0.8	456.8 ± 3.4	1.922 ± 0.01	0.745	0.44
LC1-014	9.9 ± 0.0	123.2 ± 0.8	472.0 ± 3.7	1.798 ± 0.01	0.765	0.26
LC1-021	8.7 ± 0.0	135.7 ± 0.8	371.8 ± 2.9	1.692 ± 0.01	0.703	0.48
LC1-022	6.6 ± 0.0	93.4 ± 0.7	400.5 ± 4.6	1.417 ± 0.02	0.751	0.11
LC1-029	5.8 ± 0.0	110.3 ± 0.8	290.2 ± 3.1	1.298 ± 0.02	0.722	0.35
LC1-058	13.5 ± 0.0	103.4 ± 0.8	880.4 ± 8.3	3.165 ± 0.03	0.839	0.30
LC1-061	18.0 ± 0.1	108.5 ± 0.9	1216.5 ± 11.3	4.111 ± 0.04	0.884	0.15
LC2-046	9.8 ± 0.0	78.4 ± 0.7	815.4 ± 9.3	2.848 ± 0.03	0.884	0.19
LC2-051	3.4 ± 0.0	66.3 ± 0.7	291.1 ± 5.1	1.540 ± 0.03	0.750	0.59
LC2-056	3.3 ± 0.0	64.2 ± 0.7	307.5 ± 5.6	1.914 ± 0.04	0.761	0.91
LC2-068	3.4 ± 0.0	53.8 ± 0.7	353.4 ± 8.6	1.318 ± 0.04	0.744	0.17
LC2-081	2.5 ± 0.0	69.4 ± 0.8	194.3 ± 4.5	0.985 ± 0.03	0.713	0.35
LC2-084	1.0 ± 0.0	34.8 ± 0.7	152.1 ± 7.1	0.979 ± 0.06	0.711	0.48
LC2-109	2.2 ± 0.0	87.7 ± 1.1	136.0 ± 3.0	1.116 ± 0.03	0.698	0.67
LC2-116	4.0 ± 0.0	89.5 ± 0.8	237.8 ± 3.8	0.890 ± 0.02	0.709	0.12

Results presented to 2σ level of uncertainty

[a] Rho is the associated error correlation (Ludwig, 1980)